Journal of Inorganic and General Chemistry
ZAAC
Zeitschrift für anorganische und allgemeine Chemie
www.zaac.wiley-vch.de
ARTICLE

DOI: 10.1002/zaac.201500665

Synthesis, Structures, and Fluorescent Properties of Three Cobalt-Based Coordination Polymers with a Rigid Tripodal Carboxylate Ligand

Xiao-Bin Liu,[a] Zhen-Yu Xiao,[a] Ao Huang,[a] Wen Wang,[a] Liang-Liang Zhang,[a] Rong-Ming Wang,*[a] and Dao-Feng Sun[a]

Keywords: N-donor co-ligands; Cobalt; Coordination polymers

Abstract. Three cobalt(II) coordination polymers, $[Co_2(tatb)_2(2,2'\text{-bipy})_2(H_2O)_2\cdot DMA\cdot 2H_2O]$ (**1**), $[Co_2(tatb)_2(1,10\text{-phen})_2(H_2O)_2\cdot 2H_2O]$ (**2**) and $[Co(tatb)(1,3\text{-dpp})\cdot H_2O]$ (**3**) (H_3tatb = 4,4′,4′′-(1,3,5-triazine-2,4,6-triyl)tribenzoic acid; 2,2′-bipy = 2,2′-bipyridyl; 1,10-phen = 1,10-phenanthroline; 1,3-dpp = 1,3-bis(pyridin-4-yl)propane), were synthesized solvothermally and characterized by single-crystal and powder X-ray diffraction (PXRD), as well as IR spectroscopy. Complexes **1** and **2** exhibit 1D double-chain structures, which further connect into interesting 3D networks by hydrogen bond and strong π–π interactions. Complex **3** possesses 2D 4^4-sql topology, which is packed parallel in an AA fashion. Moreover, thermal stability properties and photoluminescence properties of **1**, **2** and **3** were also investigated.

1 Introduction

In the past decades, coordination polymers (CPs) have attracted widespread interest in virtue of their fascinating structures and intriguing potential applications, such as selective molecular recognition and separation, gas storage and separation, absorption, luminescence, molecular magnet, ion-exchange and heterogeneous catalysis.[1–5] For the formation of coordination polymers, the selection of carboxylate ligand is essential. Among the family of organic carboxylate, triangular carboxylate shows more superiorities.[6–9] The ligand 4,4′,4′′-(1,3,5-triazine-2,4,6-triyl)tribenzoic acid (H_3tatb) has been utilized previously, and it has been utilized in the construction of copper coordination polymers, which possess outstanding hydrogen uptake.[10–12] Moreover, a careful selection of N-donor ligands with different conformations as secondary auxiliary ligands is a key step for the rational design of structures with specific physical and chemical properties.[13–17] However, CPs based on H_3tatb and N-donor ligands have only been investigated scarcely.

To explore the influence of N-donor ligands on achieving different dimensional and topological structures based on triangular carboxylate ligand, H_3tatb was selected as the main ligand, 2,2′-bipy, 1,10-phen, and 1,3-dpp with different conformations as co-ligands (Scheme 1). Three CPs with cobalt, namely, $[Co_2(tatb)_2(2,2'\text{-bipy})_2(H_2O)_2\cdot DMA\cdot 2H_2O]$ (**1**), $[Co_2(tatb)_2(1,10\text{-phen})_2(H_2O)_2\cdot 2H_2O]$ (**2**), and $[Co(tatb)(1,3\text{-dpp})\cdot H_2O]$ (**3**), were successfully synthesized, and characterized by single-crystal and powder X-ray diffraction, elemental analysis, IR spectroscopy, and thermogravimetry. In addition, their fluorescent properties were also investigated.

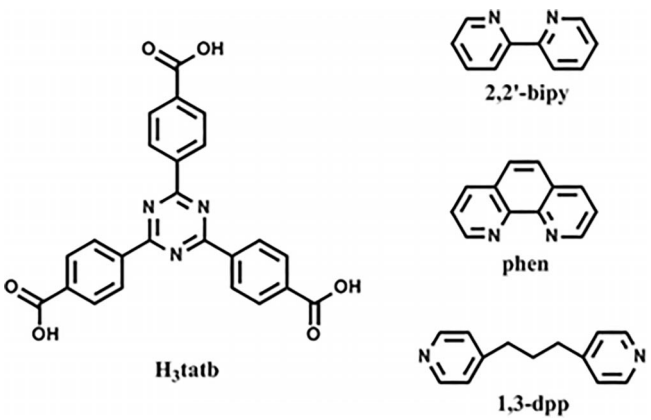

Scheme 1. Structures of H_3tatb and N-donor ligands used in this work.

2 Experimental Section

2.1 Materials and Measurements

All the reagents and solvents employed were commercially available and used as received without further purification except H_3tatb. Infrared spectra were recorded with a Bruker VERTEX-70 spectrometer as KBr pellets in the frequency range 4000–400 cm^{-1}. The elemental analyses (C, H, and N) were determined with a CE instruments EA 1110 analyzer. Luminescence spectra were recorded with a HITICHI F7000 fluorescence spectrophotometer at room temperature (25 °C). TG curves were measured from 40 to 800 °C with a METTLER TOLEDO instrument at a heating rate 10 K·min^{-1} in a nitrogen atmosphere (100 mL·min^{-1}).

* Prof. Dr. R.-M. Wang
E-Mail: rmwang@upc.edu.cn
[a] College of Science
China University of Petroleum (East China)
Qingdao, 266580, P. R. China
Supporting information for this article is available on the WWW under **http://dx.doi.org/10.1002/zaac.201500665** or from the author.

2.2 Synthesis of H_3tatb Ligand

Ligand 4,4′,4′′-(1,3,5-triazine-2,4,6-triyl)tribenzoic acid (H_3tatb) (Scheme 2) was synthesized according to the literature procedure.[10]

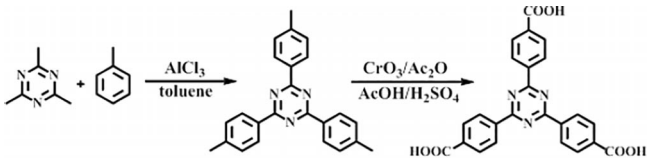

Scheme 2. The reaction pathway of H_3tatb.

2.3 Synthesis of Complexes 1–3

2.3.1 $[Co_2(tatb)_2(2,2'\text{-bipy})_2(H_2O)_2\cdot DMA\cdot 2H_2O]$ (1)

A mixture of $Co(NO_3)_2\cdot 6H_2O$ (47.9 mg, 0.114 mmol), 2,2′-bipy (33.1 mg, 0.212 mmol), H_3tatb (8.6 mg, 0.019 mmol), and 7 mL DMA-H_2O (v:v = 1:1) was sealed in a 10 mL stainless steel reactor, heated to 120 °C in 500 min, and kept at 120 °C for 4300 min. Afterwards, the reaction system was cooled to room temperature slowly at a rate of 0.1 K·min^{-1}. Purple, needle-shaped crystals were obtained and washed with DMA and dried in the air (yield: 72 %. based on cobalt). $C_{72}H_{54}Co_2N_{11}O_{16}$: calcd. C 58.92, H 3.95, N 10.50 %; found: C 57.15, H 4.05, N 11.20 %. **IR** (KBr): $\tilde{\nu}$ = 3429 (s), 2017 (w), 1639 (s), 1515 (m), 1397 (m), 1218 (w), 1106 (w), 765 (m), 591 (w) cm^{-1}.

2.3.2 Synthesis of $[Co_2(tatb)_2(1,10\text{-phen})_2(H_2O)_2\cdot 2H_2O]$ (2)

A mixture of $Co(NO_3)_2\cdot 6H_2O$ (48.0 mg, 0.165 mmol), H_3tatb (11.0 mg, 0.025 mmol), 1,10-phen (52.5 mg, 0.291 mmol), and 7 mL NMP-H_2O (v:v = 1:1) was sealed in a 10 mL stainless steel reactor and placed in an oven at 120 °C for 4300 min. Afterwards the reaction system was cooled to room temperature slowly at a rate of 0.1 K·min^{-1}. Purple crystals were obtained and washed with DMF, EtOH, and dried in the air (yield: 65 %. based on cobalt). $C_{72}H_{45}Co_2N_{10}O_{14}$: calcd. C 59.02, H 3.35, N 9.56 %; found: C 60.15, H 3.42, N 9.71 %. **IR** (KBr): $\tilde{\nu}$ = 3412 (s), 2011 (w), 1645 (s), 1509 (w), 1390 (m), 1118 (m), 1013 (w), 765 (w) cm^{-1}.

2.3.3 Synthesis of $[Co(tatb)(1,3\text{-dpp})\cdot H_2O]$ (3)

A mixture of $Co(NO_3)_2\cdot 6H_2O$ (40.9 mg, 0.141 mmol), H_3tatb (8 mg, 0.018 mmol), 1,3-dpp (22.2 mg, 0.120 mmol), and 7 mL NMP-H_2O (v:v = 1:1) was sealed in a glass tube and placed in an oven at 120 °C for 4300 min. Afterwards, the reaction system was cooled to room temperature slowly at a rate of 0.1 K·min^{-1}. Purple, needle-shaped crystals were obtained and washed with DMF, EtOH and dried in the air (yield: 70 %. based on cobalt). $C_{37}H_{23.5}CoN_5O_6$: calcd. C 62.41, H 3.50, N 9.90 %; found: C 62.55, H 3.65, N 10.21 %. **IR** (KBr): $\tilde{\nu}$ = 3435 (s), 2358 (w), 2029(w), 2024 (w), 1624 (m), 1521 (m), 1403 (m), 1131 (w), 765 (w), 585 (w) cm^{-1}.

2.4. X-ray Crystallography

Single crystals of complexes **1**–**3** with appropriate dimensions were chosen under an optical microscope and quickly coated with high vacuum grease (Dow Corning Corporation) before being mounted on a glass fiber for data collection. Data for **1**–**3** were collected with a SuperNova diffractometer equipped with a Molybdenum micro-focus X-ray sources (λ = 0.71073 Å) and an Eos CCD detector under 293 K. The data were collected with a ω-scan technique and an arbitrary ϕ-angle. Data reductions were performed with the CrysAlisPro package, and an analytical absorption correction was performed. The structures were treated anisotropically, whereas the aromatic and hydroxyl-hydrogen atoms were placed in calculated, ideal positions and refined as riding on their respective carbon or oxygen atoms. Structure was examined using the Addsym subroutine of PLATON[18] to assure that no additional symmetry could be applied to the models. Crystal data collection and parameters are summarized in Table 1, and selected bond lengths and angles are given in Table S1, Table S2, and Table S3 (Supporting Information).

Crystallographic data (excluding structure factors) for the structures in this paper have been deposited with the Cambridge Crystallographic Data Centre, CCDC, 12 Union Road, Cambridge CB21EZ, UK. Copies of the data can be obtained free of charge on quoting the depository numbers CCDC-1403528, CCDC-1403529, and CCDC-1403530. (Fax: +44-1223-336-033; E-Mail: deposit@ccdc.cam.ac.uk, http://www.ccdc.cam.ac.uk)

Table 1. Crystallographic data for **1**–**3**.

	1	**2**	**3**
Furmula	$C_{72}H_{54}Co_2N_{11}O_{16}$	$C_{72}H_{45}Co_2N_{10}O_{14}$	$C_{37}H_{23.5}CoN_5O_6$
M	1446.64	1392.04	693.07
Crystal system	triclinic	triclinic	triclinic
Space group	$P\bar{1}$	$P\bar{1}$	$P\bar{1}$
a /Å	14.0681(10)	14.6268(11)	9.0219(4)
b /Å	15.3715(10)	15.5313(11)	12.1308(9)
c /Å	17.2188(11)	17.2860(12)	16.8349(7)
α /°	107.699(6)	110.177(6)	85.216(5)
β /°	103.005(6)	100.475(6)	75.255(4)
γ /°	103.223(6)	103.126(6)	69.170(6)
V /Å^3	3274.4(4)	3441.2(4)	1665.27(16)
Z	2	2	2
D /g·cm^{-3}	1.467	1.343	1.382
μ /mm^{-1}	0.587	0.554	0.570
R_{int}	0.1198	0.0734	0.0505
GOF	0.956	0.954	1.052
R_1/ wR_2 [$I > 2\sigma(I)$]	0.0800, 0.1114	0.0775, 0.1736	0.0739, 0.2051
R_1, wR_2 (all data)	0.2393, 0.1644	0.1559, 0.2150	0.0917, 0.2275

Supporting Information (see footnote on the first page of this article): Simulated and experimental PXRD patterns, IR spectra, and selected bond lengths and angles of complexes **1**–**3**.

3 Results and Discussion

3.1 Crystal Structures

*3.1.1 [$Co_2(tatb)_2(2,2'bipy)_2(H_2O)_2$·DMA·$2H_2O$] (**1**)*

Single-crystal X-ray diffraction analysis reveals that complex **1** shows a double-strand 1D chain structure, crystallizing in the monoclinic $P\bar{1}$ space group. The asymmetric unit contains two ligands, two crystallographic independent Co^{II} ions, two 2,2′-bipy co-ligands, two coordinated water molecules, and one uncoordinated DMA molecule. As shown in Figure 1a, Co1 is hexacoordinated by three carboxylate oxygen atoms from two different $Htatb^{2-}$ molecules, one oxygen atom from coordinated water molecule, and two nitrogen atoms from 2,2′-bipy, whereas Co2 is pentacoordinated by two carboxylate oxygen atoms from two different $Htatb^{2-}$ molecules, one oxygen atom from coordinated water molecule, and two nitrogen atoms from 2,2′-bipy. The Co–O and Co–N distances range from 2.038(6) to 2.275(6) Å and 2.109(7) to 2.121(8) Å, respectively. The carboxylate ligands are partly deprotonated, and adopt μ_1-η^1-η^1 and μ_1-η^1-η^0 modes to link two different central Co^{II} atoms to form 1D double-chains, which are limited by the two chelating nitrogen atoms of central metal ions to construct higher dimensional architectures. The 1D infinite double chains are further packed into a three-dimensional supramolecular framework through π–π stacking and weak interactions. As shown in Figure 1b, the two SBUs are connected by the backbones of the H_3tatb ligands to generate two independent open frameworks with 1D channels along the *b* axis.

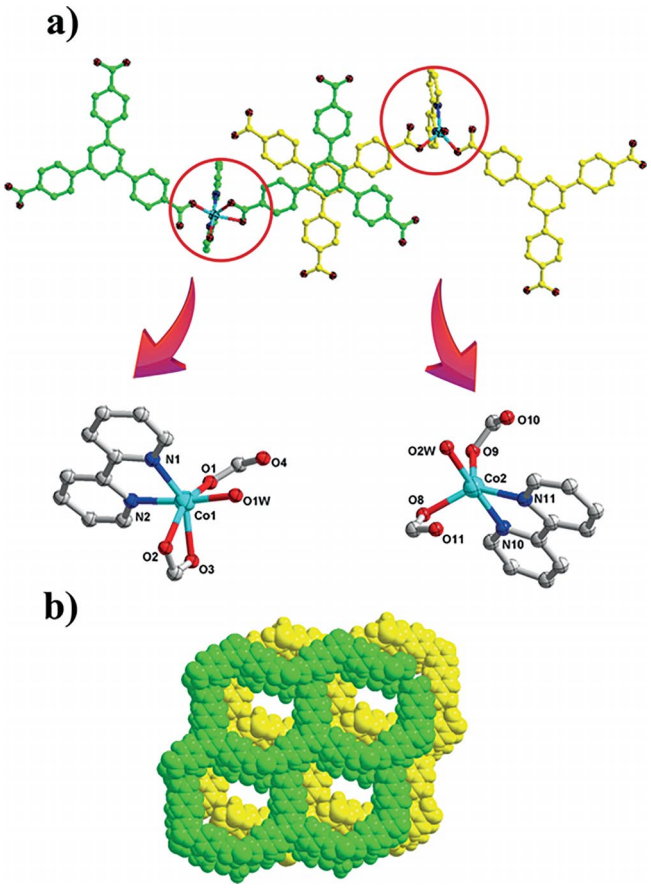

Figure 1. (a) Coordination mode of metal ions for complex **1**. (b) The 3D supramolecular architecture via π···π stacking interactions viewed from the *b* axis direction.

*3.1.2 [$Co_2(tatb)_2(1,10\text{-}phen)_2(H_2O)_2$·$2H_2O$] (**2**)*

Complex **2** crystallizes in the triclinic $P\bar{1}$ space group with a 1D double-strand framework. The asymmetric unit consists of two ligands, two cobalt ions, two 1,10-phen co-ligands, and two coordinated water molecules. The network contains two different types of single-core cobalt SBUs, and the coordination modes of two central metal atoms are the same as the instances of Co1 and Co2 in complex **1**. As shown in Figure 2a, the Co1 atom is hexacoordinated with octahedral arrangement and the Co2 atom is pentacoordinated with trigonal biyramidal arrangement. The Co–O and Co–N distances range from 2.035(5) to 2.236(5) Å and 2.098(8) to 2.148(8) Å, respectively, which is consistent with the other reported cobalt complexes.[19–22] The carboxylic groups of complex **2** also adopt μ_1-η^1-η^1 and μ_1-η^1-η^0 bridging modes to link different CoO_4N_2 and CoO_3N_2, resulting in a double-strand structure, and finally the 3D supramolecular framework is formed by π–π stacking and weak interactions.

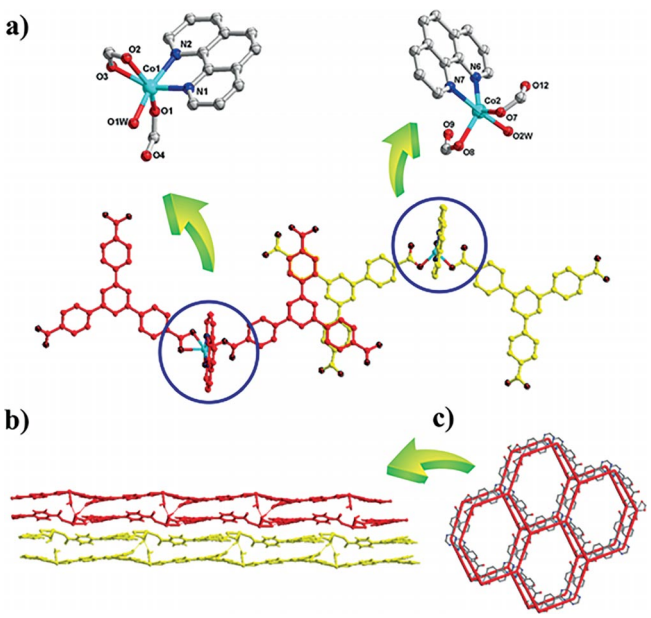

Figure 2. (a) Coordination mode of metal ions for complex **2**. (b) View of the 3D supramolecular structure and π···π stacking motifs exist in the framework. (c) View of the one Co-tatb layer simplified through topology.

*3.1.3 [Co(tatb)(1,3-dpp)·H_2O] (**3**)*

When the bridging 1,3-dpp is used instead of the chelating 2,2′-bipy or 1,10-phen ligand, complex **3** was obtained in a

good yield. X-ray single crystal diffraction displays that **3** has a 2D layer framework and crystallizes in the triclinic $P\bar{1}$ space group with 4^4-sql topology, as shown in Figure 3b and c. The asymmetrical unit contains one Co^{II} ion, one $Htatb^{2-}$ ligand, and one 1,3-dpp molecule. The coordination environment of Co^{II} ion is shown in Figure 3a. It is coordinated by four carboxylate oxygen atoms from three $Htatb^{2-}$ ligands and two nitrogen atoms from two 1,3-dpp molecules, forming a distorted octahedral arrangement. The Co–O and Co–N distances range from 2.005(4) to 2.133(4) Å and 2.114(5) to 2.166(6) Å, respectively. The carboxylic groups have two coordination modes: one carboxylate group adopts μ_2-η^1-η^1 bridging mode to link two Co^{II} ions, and another one adopts μ_1-η^1-η^1 bridging mode to link one Co^{II} ion. The 1,3-dpp molecules link two $Co_2(COO)_2$ SBUs to form 1D infinite chain, which is further connected to the final 2D layer structure by two-connected $Htatb^{2-}$ ligands, and then the adjacent 2D networks are parallel packed to 3D structure in a AA fashion, as depicted in Figure 3e and f.

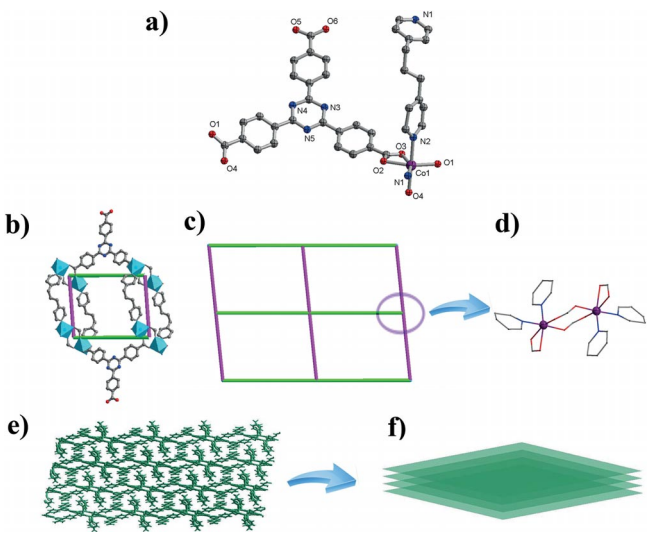

Figure 3. (a) Molecular structure of **3** with atom labeling of the asymmetric unit. (b) View of the single 2D 4^4-sql net. (c) Presentation of a 2D 4^4-sql net (d) Perspective view of the SBU. (e) 2D + 2D → 2D of the packing sheets in the crystal with a AA fashion (f) Schematic representation of the layer structure of structure **3**.

3.2 X-ray Diffraction and Thermogravimetric Analyses

The X-ray powder diffraction patterns of the samples were recorded for checking the phase purities of **1**–**3** at room temperature. As shown in Figure S1 (Supporting Information), the experimental patterns are in good agreement with simulated ones generated from the results of single-crystal diffraction data, demonstrating the phase purity of the product nicely. The preferred orientation of the crystalline powder samples perhaps caused the dissimilarities in intensity.[23]

In order to characterize the compounds more fully in terms of thermal stability, the thermogravimetric (TG) measurements were performed on polycrystalline samples of complexes **1**–**3** in a nitrogen atmosphere and the TG curves are shown in Figure 4. The three complexes show two identifiable weight loss steps. For complex **1**, the first weight loss occurs from 40 to 271 °C, which is attributed to the loss of lattice solvent molecules and the coordinated water molecules (obsd. 10.20 %, calcd. 10.99 %), then the network of **1** collapse quickly. For complex **2**, the weight loss corresponding to the release of lattice and coordination water molecules is observed from 40 to 296 °C (obsd. 5.67 %, calcd. 5.17 %), and then the framework begins to collapse, which is assigned to the decomposition of 1,10-phen and H_3tatb ligands. For complex **3**, the loss of lattice water molecules (obsd. 2.80 %, calcd. 2.60 %) is observed before 201 °C, and then the abrupt weight loss is assigned to the decomposition of organic ligands.

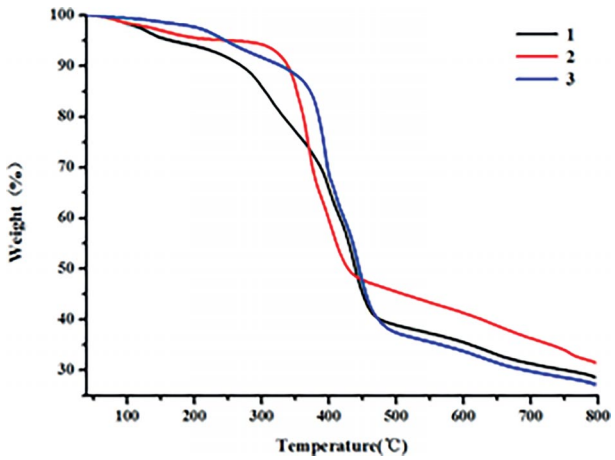

Figure 4. TGA curves of complexes **1**–**3**.

3.3 Photoluminescence Properties

The luminescent emission spectra of complexes **1**–**3** were examined in the solid state at room temperature as is shown in Figure 5. The main emission peak of the free rigid ligand tatb appears at 443 nm (λ_{ex} = 330 nm) and can be assigned to the intra-ligand π*–π transitions.[24,25] Complexes **1**–**3** show similar emission peaks at 434 nm, 438 nm, and 436 nm, respec-

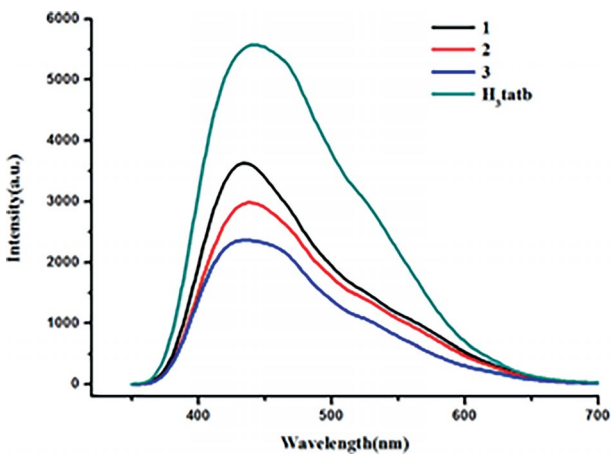

Figure 5. Solid-state fluorescence emissions of complexes **1**–**3**, and H_3tatb.

tively, which are attributed to ligand-based charge transfer as they only display small shifts when comparing to the position of ligand peak.

4 Conclusions

Three Co^{II} coordination polymers based on 4,4′,4′′-(1,3,5-triazine-2,4,6-triyl)tribenzoic acid (H_3tatb), and different types of N-donor co-ligands (2,2′-bipy, 1,10-phen, and 1,3-dpp) are synthesized. Complexes **1** and **2** exhibit 1D double-chain structure owing to the influence of chelate auxiliary ligands (2,2′-bipy and 1,10-phen), whereas complex **3** shows 2D 4^4-sql network in virtue of the bridging effects of 1,3-dpp. The luminescent spectra of complexes **1**–**3** display ligand-based photoluminescence.

Acknowledgements

This work was supported by the National Natural Science Foundation of China (grant no. 21371179), and Fundamental Research Funds for the Central Universities (13CX05010A, 14CX02158A).

References

[1] B. Zheng, J. Bai, J. Duan, L. Wojtas, M. J. Zaworotko, *J. Am. Chem. Soc.* **2010**, *133*, 748–751.
[2] Z. M. Hao, X. Z. Song, M. Zhu, X. Meng, S. N. Zhao, S. Q. Su, W. T. Yang, S. Y. Song, H. J. Zhang, *J. Mater. Chem. A* **2013**, *1*, 11043–11050.
[3] K. S. Jeong, Y. B. Go, S. M. Shin, S. J. Lee, J. Kim, O. M. Yaghi, N. Jeong, *Chem. Sci.* **2011**, *2*, 877–882.
[4] Z. J. Lin, J. Lv, M. C. Hong, R. Cao, *Chem. Soc. Rev.* **2014**, *43*, 5867–5895.
[5] J. R. Li, J. Sculley, H. C. Zhou, *Chem. Rev.* **2012**, *112*, 869–932.
[6] M. P. Suh, H. J. Park, T. K. Prasad, D. W. Lim, *Chem. Rev.* **2012**, *112*, 782–835.
[7] Y. W. Li, H. Ma, Y. Q. Chen, K. H. He, Z. X. Li, X. H. Bu, *Cryst. Growth Des.* **2012**, *12*, 189–196.
[8] J. P. Zhang, Y. B. Zhang, J. B. Lin, X. M. Chen, *Chem. Rev.* **2012**, *112*, 1001–1033.
[9] H. L. Wang, D. P. Zhang, D. F. Sun, Y. T. Chen, K. Wang, Z. H. Ni, L. J. Tian, J. Z. Jiang, *CrystEngComm* **2010**, *12*, 1096–1102.
[10] D. F. Sun, S. Q. Ma, Y. X. Ke, D. J. Collins, H. C. Zhou, *J. Am. Chem. Soc.* **2006**, *128*, 3896–3897.
[11] D. F. Sun, S. Q. Ma, Y. X. Ke, T. M. Petersen, H.-C. Zhou, *Chem. Commun.* **2005**, *2663*, 2665.
[12] D. F. Sun, Y. X. Ke, D. J. Collins, G. A. Lorigan, H. C. Zhou, *Inorg. Chem.* **2007**, *46*, 2725–2734.
[13] Z. J. Lin, D. S. Wragg, J. E. Warren, R. E. Morris, *J. Am. Chem. Soc.* **2007**, *129*, 10334–10335.
[14] M. H. Mir, L. L. Koh, G. K. Tan, J. J. Vittal, *Angew. Chem. Int. Ed.* **2010**, *49*, 390–393.
[15] S. M. Fang, M. Hu, Q. Zhang, M. Du, C.-S. Liu, *Dalton Trans.* **2011**, *40*, 4527–4541.
[16] Q. X. Jia, H. Tian, J. Y. Zhang, E. Q. Gao, *Chem. Eur. J.* **2011**, *17*, 1040–1051.
[17] L. J. Murray, M. Dinča, J. R. Long, *Chem. Soc. Rev.* **2009**, *38*, 1294–1314.
[18] S. Ding, X. Sun, Y. Zhu, Q. Chen, Y. Xu, *Acta Crystallogr. Sect. A* **2006**, *62*, i269-i271.
[19] D. M. Chen, X. Z. Ma, X. J. Zhang, N. Xu, P. Cheng, *Inorg. Chem.* **2015**, *54*, 2976–2982.
[20] L. L. Zhang, F. L. Liu, Y. Guo, X. P. Wang, J. Guo, Y. H. Wei, Z. Chen, D. F. Sun, *Cryst. Growth Des.* **2012**, *12*, 6215–6222.
[21] F. L. Liu, L. L. Zhang, R. M. Wang, J. Sun, J. Yang, Z. Chen, X. P. Wang, D. F. Sun, *CrystEngComm* **2014**, *16*, 2917–2928.
[22] L. Y. Zhang, J. P. Zhang, Y. Y. Lin, X. M. Chen, *Cryst. Growth Des.* **2006**, *6*, 1684–1689.
[23] L. Qin, M. Zhang, Q. Yang, Y. Li, H. Zheng, *Cryst. Growth Des.* **2013**, *13*, 5045–5046.
[24] Y. Gong, Z. Hao, J. L. Sun, H.-F. Shi, P.-G. Jiang, J.-H. Lin, *Dalton Trans.* **2013**, *42*, 13241–13250.
[25] G. Tian, G. S. Zhu, Q. R. Fang, X. D. Guo, M. Xue, J. Y. Sun, S. L. Qiu, *J. Mol. Struct.* **2006**, *787*, 45–49.

Received: August 30, 2015
Published Online: November 13, 2015

